King Saud University

Arabian Journal of Chemistry

www.ksu.edu.sa
www.sciencedirect.com

REVIEW ARTICLE

Recent advances on hydrogels based on chitosan and alginate for the adsorption of dyes and metal ions from water

Mohammad T. ALSamman, Julio Sánchez *

Universidad de Santiago de Chile (USACH), Facultad de Química y Biología, Departamento de Ciencias del Ambiente, Santiago, Chile

Abstract In contemporary times, water resources have become increasingly scarce and suffer from anthropogenic pollution sources with an organic and inorganic origin that are products of industrial, agricultural, and everyday waste. Contamination with heavy metals and dyes in wastewater is considered a risk for water sources that can leak into underground and surface sources, leading to increased biological and chemical contamination. The pollutant removal process is performed by adsorption treatment methods, which is the most common method, and it is considered an effective method with a high and economical removal rate.

In this review, we discuss the use of biobased hydrogel adsorbents in the removal of organic dyes and metal ions from water. The literature indicates that hydrogels exhibit rapid absorption kinetics and a dye removal absorption capacity that can reach more than 100 mg/g and sometimes more than 2000 mg/g, with a metal adsorption capacity ranging from 38 mg/g to more than 440 mg/g. These results are discussed and compared by taking into account hydrogel materials that contain biopolymers such as alginate, chitosan or both. In general, absorption depends mainly on biobased materials, which have a natural origin and can be utilized to synthesize hydrogels to remove pollutants, dyes and heavy metals. Chitosan and alginate are prominent materials for this use and they can be incorporated with other components to obtain hydrogels or nanocomposite materials with different efficacies to remove dyes and metal ions.

© 2021 The Author(s). Published by Elsevier B.V. on behalf of King Saud University. This is an open access article under the CC BY-NC-ND license (http://creativecommons.org/licenses/by-nc-nd/4.0/).

* Corresponding author.
E-mail address: julio.sanchez@usach.cl (J. Sánchez).
Peer review under responsibility of King Saud University.

Production and hosting by Elsevier

Contents

1. Introduction

The scarcity of water resources is increasing worldwide due to the increasing imbalance between the availability and consumption of freshwater. An increased population and migration to drought-prone areas due to rapid industrial development, increased per capita water use, and climate change has led to changing weather patterns in populated areas (Ta Wee Seow et al, 2016). Water pollution is a global problem that threatens the entire biosphere and affects the lives of many millions of people around the world. Water pollution is not only one of the most important global risk factors for disease and death but also contributes to the continual reduction in available drinking water around the world (Sreenath Bolisetty et al. 2019).

Chile suffers from drought, as many cities and towns suffer from water scarcity and impurities, such that experienced by most Arab Gulf countries and third world countries. In addition to rapid industrial growth, global warming is leading to unnatural climate changes and uncontrolled groundwater development. This leads to desertification and drought and affects the sensory specifications of industrial products. Therefore, water treatment must be carried out at the best cost, as many countries are unable to bear the high cost of the indus-try, as countries must maintain food security and industrial security (Kia, A., et al., 2017). There are different types of materials (e.g., nanomaterials), which have tremendous potential for treating polluted water very effectively due to their unique properties, such as a larger surface area and ability to work at low concentrations.

Most metal heavy metal ions in water can lead to high toxicity towards aquatic life, plants, animals, human beings, and the environment and can be easily removed due to their absorption by organic systems and organisms (Okereafor, U et al. 2020). On the other hand, dyes are split into many types, such as azo, mordant, vat, acidic and basic dyes, which contain chromophores, auxochromes, and chromogens (Ziarani, G. M., et al. 2018; Clark, M. ed., 2011).

Polysaccharides, such as alginate or chitosan, are abundant and are widely applied in water treatment (Ibrahim, N. A et al. 2018). However, some polysaccharides have poor mechanical, chemical and physical properties, and, therefore, they are often modified with various synthetic or natural monomers and combined with many materials for the purpose of application in water treatment (Mittal, H., Ray, S.S. and Okamoto, M., 2016).

Therefore, developing cheaper, more efficient, biodegradable and more environmentally friendly adsorbents is a must

such as, for example, the production of bioadsorbents from renewable resources such as low-cost sorbent hydrogels. (De Gisi, S et al. 2016; Pérez-Álvarez et al., 2019; Godiya et al., 2020a; Godiya et al., 2020b). In addition to bioadsorbents, such as biobased hydrogels, show higher adsorption capacity, as these bioadsorbents are more hydrophilic, low-cost, show biodegradability, high efficiency, minimization of chemical or biological sludge, and good reusability (Crini, G., 2005; Akter, M et al. 2021, Van Tran, V et al., 2018). Additionally, biobased hydrogels can swell in water and simultaneously produce separation of heavy metal ions and dyes (Shalla, A. H et al. 2019).

In general, alginate and chitosan biopolymers can be incorporated into composite materials such as interpenetrating polymer networks (IPNs), semi-IPNs, networks obtained by grafting polymerization, nanocomposites obtained by incorporation of metals (or metal oxides), nanocomposites of carbon-derived materials, and incorporation of natural nanomaterials to produce advanced adsorbents (Dragan, E. S et al. 2012; Bashir, S et al. 2020; Zubair, M. and Ullah, A., 2021).

2. Water contamination of dyes and metal ions

2.1. Types of water

Natural water is commonly divided into surface water and groundwater. Surface water includes lakes, reservoirs, ponds, rivers, and streams, which each have their own dynamics and are exposed to both the underlying terrestrial surfaces and the atmosphere.

Water can contain toxic compounds such as metals, metalloids, and organic compounds. Pollution is defined by the presence and concentration of these components and depends greatly on the type and size of the water body. Water considered unfit for human drinking can be suitable for other uses, such as irrigation and other works (L. Schweitzer, J. Noblet, 2018).

2.2. Sources of water pollution

Pollution sources are divided and branched into fixed sources and nonspecific sources. Fixed sources are sources with a hard and fast location and an area of permanent pollution that is constantly being polluted, such as power plants, refineries, mines, sewage treatment plants, etc. Unspecified and nonpoint sources are sources that are distributed over a good geographical region and do not have a selected location and an indeterminate pollutant, such as watersheds. Unspecified sources may include mobile sources such as cars, buses, and trains (L. Schweitzer, J. Noblet, 2018).

Wastewater pollution with heavy metals is the largest environmental problem and poses human endangerment worldwide thanks to rapid urbanization and industrialization, such as metallic paint, mining, tanneries, coatings, batteries, paper industries, printing and imaging industries, pesticides, fertilizers, and the manufacturing of automobile radiators. Heavy metal ions such as As(III), As(V), Pb(II), Cd(II), Ni(I), Cr(III), Cr(VI), Zn(II), Cu(II), Hg(I), Hg(II), and Co(II), among others, can be present in wastewater (Mahmud et al. 2016).

Wastewater from textile industries is often a threat to the environment in an exceedingly large part of the planet. From an environmental point of view, the textile industry is one of the foremost polluting industries in the world due to its enormous consumption of water (in some cases up to 3000 m^3/day). The use of harmful chemicals, high consumption water and energy, generation of large quantities of large solid and gas waste fuel consumption for transportation to remote locations where textile units are located determine the placement and use of nondegradable packaging materials (Choudhury, A.R., 2014). The effluent from the textile industry is closely associated with the characteristics of the textile product, the standard, the origin of the raw materials (wool, cotton, linen, and artificial fibres), the chemicals that aid the dye, and, additionally because of the inner pollution prevention and process management strategies there are severe fluctuations within the factors (K. Sarayu & S. Sandhya, 2012).

3. Chitosan-based hydrogels to remove metal ions and dyes

Hydrogels form three-dimensional structures that are cross-linked network structures with a swelling ability in water or another solvent without dissolving due to their moisture content, excellent flexibility, and outstanding viscoelasticity. However, the polymer used for preparing the hydrogel must meet the subsequent conditions: first, the characteristic network structure, such as the distinct network, chemical structure, and aggregate structure, which can affect the water absorbability of the polymer, via the swelling rate of the synthesized hydrogels, and different methods can also be used to prepare hydrogels including impregnation, grafting, crosslinking, chelation and in situ polymerization (Y. Wang et al, 2018).

Based on Fig. 1 the types of hydrogel chitosan can be classified generally as follows:

3.1. Interpenetrating polymer networks (IPNs) and semi-interpenetrating polymer network (semi-IPN) chitosan hydrogels

As chitosan is polysaccharide with structure of linear cationic formed by b-(1 / 4)-2-amino-2- deoxy-D-glucopyranose and b-(1 / 4)-2-acetamido-2-deoxy-D-glucopyranose units, while most of hydrogels types containing chitosan are obtained by polymerization or copolymerization of chitosan with other polymer types, such as synthetic polymers or natural polymers, while using crosslinkers or several crosslinkers to form full IPNs or several semi-IPN, while the semi-IPN and full IPN-type hydrogels can be obtained by varying the initiator and crosslinker concentrations, which can differ in the crosslinking degree and chitosan mass ratio (see Fig. 2). Which can be classified to covalent semi-IPN, noncovalent semi-IPN, noncovalent full-IPN, sequential IPN, simultaneous IPN, latex IPN, thermoplastic IPN and gradient IPN.

As the covalent semi-IPN formed unglued to two cross-linked polymeric systems as single polymeric network, while the noncovalent semi-IPN are only one crosslinked polymeric system (see Fig. 3).

These hydrogels are optimistic for the removal of anionic dyes such as methyl violet and Congo red, and for other industrial dyes from water or solvents, which can be defined by
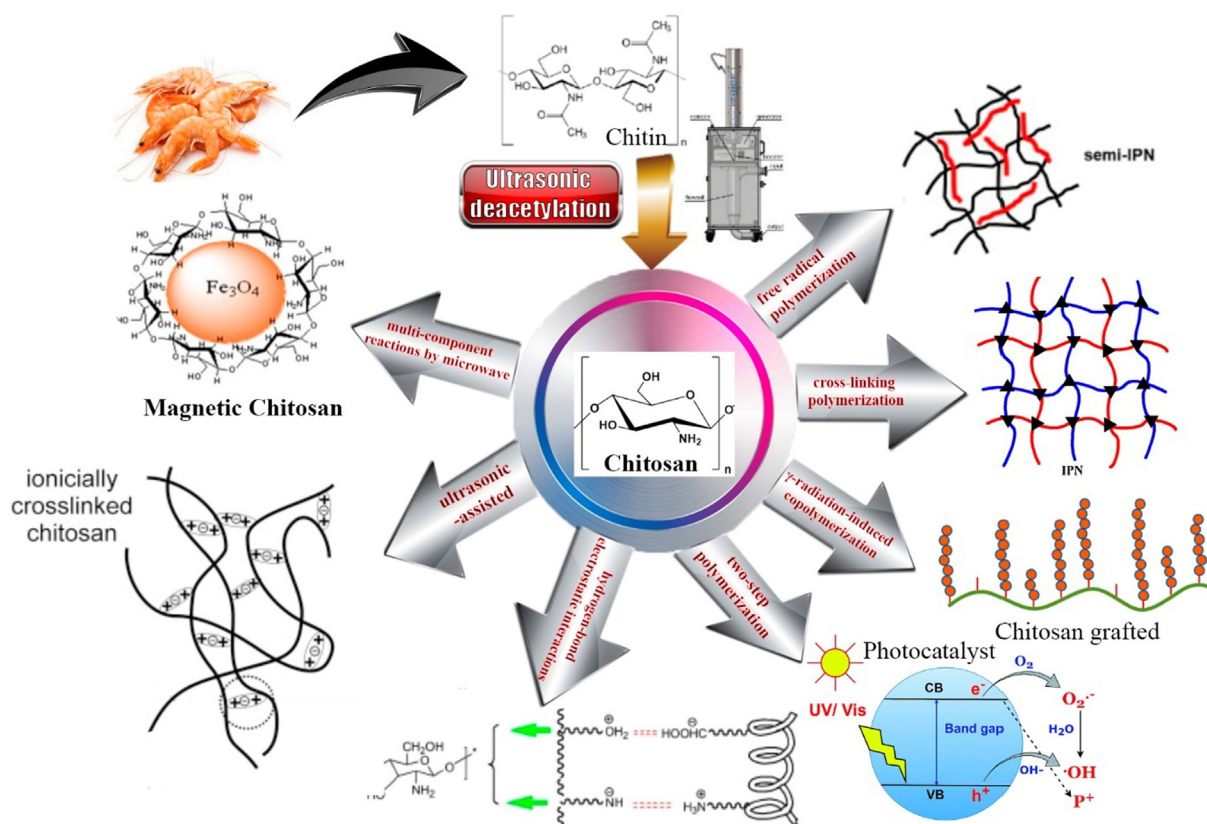
Fig. 1   Chitosan nanocomposite types and preparation method used for dye and metal removal.

studying the mechanism and isotherm (Maity and Ray, 2014; Silverstein, M.S., 2020; Zoratto, N. and Matricardi, P., 2018).

Other study based on polyacrylamide (PAAm) and chitosan (CS) offers an explanation of the strong differences between s-IPN and IPN regarding swelling and interaction with mandaline dyes is provided by the structural changes that occur during formation of the second lattice at high pH, when a fraction is transformed from amide groups into carboxyl groups by primary hydrolysis, thus generating an amphoteric IPN hydrogel. In one step, s-IPN hydrogels were synthesized on the basis of PAAm and CS by cross-linking AAm polymerization in the presence of CS. Adsorption stains on s-IPN1.60 and d-IPN2.60. D-IPNs is higher. Mixing chitosan with other biopolymers has been shown to be an effective way to enhance water resistance and enhance stability within water during the absorption process (Cui, L et al. 2014).

The semi- IPN is defined as follows: an IPN is a polymer containing one or more networks and one or more linear or branched polymer(s), which are characterized by infiltration on a molecular scale and the properties of the networks and linear or branched macromolecules can be determined by spectroscopy (Zoratto, N. and Matricardi, P., 2018). As an example, Ngwabebhoh. F. A. and his research group obtained a superabsorbent chitosan-starch (ChS) hydrogel that includes electrostatically different charge interactions between anionic sulfonyl (-SO$_3$ $^-$) groups of dissolved DR80 dye and protonated amino (–NH$_3^+$) groups of chitosan boosted by hydrophobic/hydrophilic interactions, and the results show an adsorption capacity of 312.77 mg/g, obtaining an economical, inexpensive, nontoxic hydrogel that has an absorbent

capacity with a high absorption efficiency of 83.5% and is also environmentally friendly. This hydrogel can be used for absorption in all solutions, wastewater, and water (Ngwabebhoh et al 2016). Wen-Bo Wang et al. synthesized a semi-IPN hydrogel based on chitosan and gelatine, and semi-IPN hydrogels were prepared in situ in an aqueous solution by grafting free radicals and crosslinking reactions between chitosan (CTS), acrylic acid (AA), gelatine (GE), and N,N-methylene bis-acrylamide. For Cu (II) ion hydrogels, the results indicate that the hydrogel containing 2 wt% GE has the highest absorption capacity of 261.08 mg/g with a recovery rate of 95.2%. Incorporating 10 wt GE boosted the storage modulus by 103.4% (ω = 100 rad/s) and 115.1% (ω = 0.1 r ad/s) and the adsorption rate by 5.67%. Moreover, the absorption capacity of the hydrogel remained as high as 153.9 mg/g after five cycles of adsorption - absorption. It was found that the ion exchange reactions between the functional groups (–COO$^-$ and –NH$_2$) of the aqueous gels are complex and that these hydrogels have the ability to be reused and recovered (Wang et al. 2013).

3.2. Grafted chitosan hydrogels

The hydrogel was prepared by polymerization of polyacrylamide grafted onto chitosan crosslinked with N,N′-methylene bis-acrylamide, whereas the grafting leads to a mild structure and increased molecular weight for the copolymer and an increase in the number of charges (Zhao, N et al 2020). The hydrogel was synthesized by conventional and

microwave-assisted methods. The maximum adsorption capacity (255.5 mg/g) of microwave prepared compared with the conventional capacity (151.7 mg/g) and the adsorption efficiency of the microwave synthesized gel was 96.9 $\pm$ 0.2% less than that obtained for the synthesized conventional gel (99.1 $\pm$ 0.2%) (R. C. da silva et al. 2020).

3.3. Photocatalytic chitosan hydrogels

Photocatalytic processes are inexpensive, environmentally friendly, and suitable for adsorption (MN Chong et al. 2010.). J. Zhou el al. synthesized a nano-TiO_2/chitosan/poly(N-isopropylacrylamide) (nano-TiO2/CS/PNIPAAm) composite hydrogel prepared by a two-step polymerization method; the use of nano-TiO_2, which contains the efficacy photocatalytic activity with the ability to absorb AF dyes, increased the removal rate from 64.02% to 90.80% under UV irradiation from 60 min to 150 min (Zhou et al. 2017). R. Jiang et al. synthesized a nano-ZnO/chitosan hydrogel with photocatalysis under solar light irradiation. The sensitized colloidal CdS nano-ZnO/chitosan (CdS@n-ZnO/CS) hydrogel was designed to realize photocatalytic activity for CdS@n-ZnO/CS and was evaluated with the photodegradation of azo dye (CR). Studies of biofunctionalized CdS@n-ZnO/CS hydrogel that show high photocatalytic activity have even shown that hydrogel has the power to transfer electrons, remove dyes and can be employed in real applications for the ultra-fast treatment and purification of dye-containing wastewater within the presence of solar light (Jiang et al. 2021).

In other study, nanocomposite hydrogels were obtained by γ-radiation-induced copolymerization, known as the gamma irradiation technique, which involve crosslinking of chitosan biopolymer (CS), acrylic acid (AAc) and TiO_2 nanoparticles (CS-PAAc/TiO_2). Theis hydrogel was used to remove methylene blue (MB) dye from aqueous solution, and the results showed that CS-PAAc/TiO_2 nanocomposites ranked with high adsorption capacity towards MB reaching 0.20 g per liter (Mahmoud et al. 2020).

3.4. Ion exchanger chitosan hydrogels

The hydrogel based on the chitosan-gelatine ion exchanger has high selectivity, and the addition of metallic elements such as zirconium (IV) leads to a positive charge that is affected by the anionic dyes. The addition of selenophosphate leads to selectivity for cationic dyes. As the MB absorption efficacy of the materials increased (99% from 12%), the adsorption process followed Langmuir adsorption (Q_o = 10.46 mg^{-1}) and a nonlinear PFO kinetic model with k1, qe (calculated), R2, RMSE = 0.011, 1.02 (mg.g^{-1}), 0.996, and 0.01709, respectively, with significant degradation (99%) of MB within 3 h of photoirradiation with a maximum adsorption capacity of 10.46 (mg g^{-1}) (K. Kaur, R. Jindal, 2019).

3.5. Crosslinked chitosan hydrogels

Graphene is usually derived from coal and methods for preparing the graphene oxide film are reviewed, including vacuum suction filtration, spray coating, spin coating, dip coating and the layer-by-layer method, and the oxidized graphite (GO) can be obtained by heating and chemical reduction. H. Mittal et al. prepared graphene oxide, chitosan and carboxymethyl cellulose (CS/CMC-NCH)-crosslinked nanocomposite hydrogels that were synthesized as adsorbents for the remediation of water. The hydrogels were made to absorb anionic (methyl orange, MO) and cationic dyes (methylene blue, MB) contaminated in wastewater or water. Approximately 99% of the dye was adsorbed from a 50 mg/L MB dye solution at 0.4 g/L by using the CS/CMC-NCH hydrogel at pH 7, and the MO absorption efficacy was approximately 82% as the dye was adsorbed at 0.6 g/L by using the CS/CMC-NCH hydrogel at pH 3 (Mittal et al. 2021).

In other study R. R. Mohamed successfully synthesized physically crosslinked hydrogels N-quaternized chitosan/poly (acrylic acid) manufactured from the following materials, N, N,N-trimethyl chitosan chloride (N-quaternized chitosan) and poly(acrylic acid), with different weight ratios (3:1), (1:1) and (1:3). These hydrogels are denoted with the following codes: Q3P1, Q1P1, and Q1P3, respectively. When using chitosan, the maximum adsorption capacity for the metals Cr (III), Fe(III), Ni(II), Cu(II), Cd(II) was only 332.0 mg/g, 355.4 mg/g, 647.2 mg/g, 677.2 mg/g and 1095.2 mg/g, when using the Q1P3 hydrogel, the maximum adsorption capacity was 275.9 mg/g, 599.5 mg/g, 398.0 mg/g, 503.2 mg/g and 1261.7 mg/g, when using the Q1P1 hydrogel, the maximum adsorption capacity was 269.5 mg/g, 315.0 mg/g, 452.0 mg/g, 521.5 mg/g and 1198.5 mg/g, and when using Q3P1 hydrogel, the maximum adsorption capacity was 233.5 mg/g, 115.0 mg/g, 398.8 mg/g, 507.6 mg/g and 1197.7 mg/g, respectively (Mohamed et al. 2017).

Cross-linked oxalic acid/chitosan hydrogels have been manufactured and studied for their azo dye absorbing properties Reactive Red 195 (RR195), wherein a difference in the charge leads to interactions between protonated amino groups of chitosan and oxalate ions, where the surface properties are studied for adsorption/desorption operations to analyse specific areas. The difference in charge leads to electrostatic interactions between protonated amino groups of chitosan and oxalate ions, leading to an increase in the absorption and an increase in the absorption efficiency as the percentage of dye removal by the biosorbent shows a maximum value of removal of 90.6% with an adsorption capacity of 114 mg/g at pH = 4 (Pérez-Calderón et al. 2020).

In another study, porous material adsorbents are formed in the presence of salicylaldehyde linked to chitosan to remove toxic dyes, showing excellent surface porosity. These porous properties contribute to the absorption of dyes such as Rose Bengal in acidic aqueous solution (pH 4) and crystal violet in neutral solution (pH 6). Chitosan-salicylaldehyde has an absorbent efficacy that ranges from 98% and 99% at room temperature. In addition to its porous properties, the dye absorption depends on stronger interactions, i.e., H-bonding, electrostatic interaction, and π-π interaction between the hydrogel and the functional groups of the dye (Parshi et al. 2019).

3.6. Magnetic chitosan hydrogels

Magnetic chitosan/poly(vinyl alcohol) hydrogel beads (m-CS/ PVA HBs) were synthesized by using an instantaneous gelation method without prejudice and loss of crystal structure shape of Fe_3O_4. The addition of metallic Fe_3O_4 nanoparticles

can increase the saturation magnetization (21.96 emu g^{-1}) of m-CS/PVA HBs compared to other magnetic bioadsorbents and can increase the adsorption capacity of Congo red onto m-CS/PVA HBs to 470.1 mg g^{-1} (Zhu et al. 2012).

The addition of elements such as magnetic graphene oxide nanoparticles (GO/Fe$_3$O$_4$) with magnetic properties increases the selectivity and increases the removal efficiency in aqueous media, as these materials also result in an increase in chemical stability that leads to a steady state. This element (GO/Fe$_3$O$_4$) was added to create magnetic chitosan hydrogel beads based on chitosan (75–85% degree of deacetylation, Mw = 200 kDa) and isophthaloyl chloride via interfacial polymerization to study the absorption and removal properties of cationic and anionic dyes from aqueous solution, and the results showed that the maximum adsorption capacities of cationic MB and anionic EBT were 289 mg/g and 292 mg/g, respectively (Mahsa Jamali & Ahmad Akbari, 2021).

In addition, chitosan hydrogels can be grafted; for example, chitosan-based hydrogel, graft co-polymerization with methylene bisacrylamide and poly(acrylic acid), (for example, CS-co-MMB-co-PAA), demineralization pH between 4.5 and 5.5, and initial mineral concentration of 300 mg dm^{-3} with 100 mg of dried hydrogel mass, achieving a recovery of 97% for Cd (II) and 94% for Pb (II) or Cu (II) ions with a Pb (II), Cd(II) and Cu(II) ion adsorption capacity of 163.90 mg/g, 135.51 mg/g and 152.42 mg/g, respectively (Paulino et al. 2011).

Activated carbon, which is usually derived from charcoal but is now derived from chitosan hydrogel coated with tea saponin due to its own surface, permits the removal and adsorption of dyes using methylene blue as a model dye and reaches a maximum adsorption capacity of 604.10 mg/g. The total pore volume of the hydrogel reaches 6.039 cm^3/g, and a maximum adsorption capacity of only 123.52 mg/g (Ma et al. 2021).

3.7. Natural materials to prepare chitosan hydrogels

This hydrogel is made with sugar and polysaccharide natural ingredients, such as glucose and chitosan hydrogel (GC hydrogel), using an initiator and a crosslinking agent by an ultrasonic-assisted method. This hydrogel was successfully synthesized and applied to adsorb Co(II) in wastewater. The results showed that GC hydrogels had adsorption capacities of 202 mg g^{-1} for Co(II) at 20 °C, pH = 7 and an adsorbent dosage of 0.01 g (Liu et al. 2019).

A xanthate-modified chitosan/poly(N-isopropylacrylamide) compound hydrogel was synthesized in an easy two-step method for selective absorption of Cu(II), Pb(II), and Ni(II) metal ions from aqueous solutions and manufactured for selective adsorption of Cu(II), Pb(II) and Ni(II) from aqueous solutions. The maximum absorption capacities for Co(II), Pb(II), and Ni(II) at 293 K were approximately 115.1 mg.g^{-1}, 172.0 mg g^{-1} and 66.9 mg g^{-1}, respectively (Wu et al. 2018).

Polydopamine-modified chitosan (CS-PDA) aerogels were synthesized through dopamine self-polymerase and glutaraldehyde binding reactions to enhance adsorption capacity and acidic chitosan resistance. The maximum adsorption capacities of CS-PDA for Cr(VI) and Pb(II) were 374.4 mg/g and

441.2 mg/g, respectively. After eight cycles, the CS-PDA absorption capacity showed no apparent reduction, excellent economic feasibility and reusability (Guo et al. 2018).

3.8. Clays/chitosan hydrogels

Montmorillonite (Mt) is a phyllosilicate mineral that contains a layered nanostructure (layers with a thickness of 1 nm) with each layer consisting of one O-Al(Mg)-O bond and two O-Si-O bonds and composed of tetrahedral sheets and octahedral sheets (approximately 100 nm × 100 nm in width and length) that impart a porous structure with high adsorption and selective absorption of dyes and metal ions. The treatment proceeds via by Van der Waals forces and electrostatic forces, and the adsorption proceeds through an ion exchange reaction. As wastewater contains the mineral elements Na$^+$, Ca^{2+}, Br$^-$, Cl$^-$ and organic cations (Zhou et al., 2019). W. Wang et al. synthesized poly(vinyl alcohol)-sodium alginate-chitosan-montmorillonite nanosheets (MMTNS), where the structure is based on hydrogen bonds and electrostatic interactions at high pH values due to the high electronegativity resulting from the deprotonation of hydroxyl groups. These hydrogels, due to the presence of clay and chitosan, lead to stability and reusability, and the MB removal rate for the hydrogel beads was 90% after 250 min when using MMTNS at an amount of 29.70% (W. Wang et al. 2018).

W. Wang et al. synthesized a carboxymethyl cellulose-chitosan system to synthesize an absorbent material with porous properties that is thermodynamically stable and has the ability to absorb dyes thanks to the porosity of the structure. These materials was successfully synthesized via hydrogen bonding of the montmorillonite with –NH$_2$ of the chitosan, as amidation and chains produce interactions to reveal a high MB removal rate of 97%, which was achieved via use of 0.2 g/L hydrogel within 360 min (Wang et al. 2020).

Chitosan/acid-activated montmorillonite composites and chitosan-based hydrogels were synthesized by copolymerization of radical chitosan, acrylic acid and N,N′-methylene bis-acrylamide. Absorption was studied for metal ions such as Pb(II) and Ni(II), and the results showed that chitosan-based hydrogels had adsorption capacities ranging from 41.06 mg/g and 30.20 mg/g. After adding montmorillonite, the adsorption capacity increased to 42.38 mg/g and 36.45 mg/g for dried hydrogels in the pH range of 5.5–3.5, respectively (Vieira et al. 2018).

Bentonite clay, chitosan, and acrylic copolymer gel hydrogels were successfully synthesized by free radical polymerization in the presence of N,N-methylene bis-acrylamide as a crosslinker, which has been separately reported and used for the adsorption of dyes. Bentonite is an inorganic material adsorbent. Montmorillonite is the main ingredient, which consists of two layers of sandwiching tetrahedral silica sheets, and the hydrogel adsorption capacity reaches 93–492 mg/g for malachite green and 91.6–482 mg/g for methyl violet dye with an efficient removal efficiency of 75–96.5% for malachite green dye and 73.5–93% for methyl violet dye (Bhattacharyya and Ray, 2014).

Table 1 shows the classification of chitosan hydrogels and their adsorption conditions and performances.

Table 1 Classification of chitosan hydrogels and their adsorption conditions and performances.

Adsorbent	Adsorbate	Adsorption capacity (mg/g)	pH - Temperature (°C)	Reference
1. Hydrogels used for dyes removal				
Salicylaldehyde linked chitosan	Crystal violet	6.85 mg/g	pH 6.0–30 °C	(N. Parshi et al. 2019)
	Rose bengal	15.26 mg/g	pH 4.0–30 °C	
Chitosan-Gelatin-Zr(IV)	Methylene blue	10.46 mg/g	pH 7.0–30 °C	(K. Kaur, R. Jindal, 2019)
Chitosan/oxalic acid	Azo dye-Reactive Red 195	110.7 mg/g	pH 4.0 – 25 °C	(J. Pérez-Calderón et al. 2020)
Chitosan/polyacrylate/graphene oxide	Methylene blue FY3	296.5 mg/g 280.3 mg/g	pH 5–9 – 25 °C	(Z. Chang et al. 2020)
β-cyclodextrin/chitosan/GO	Methylene blue	230.29 mg/g	pH 12 – 25 °C	(Y. Liu et al. 2018)
Chitosan/cellulose	Congo red	380 mg/g	25 °C	(Hu tu et al. 2017)
GO - chitosan/carboxymethyl cellulose	Methyl orange Methylene blue	404.52 mg/g 655.98 mg/g	pH 3.0 – 25 °C pH 7.0–25 °C	(H. Mittal et al. 2021)
Exfoliated montmorillonite nanosheets (MMTNS)/chitosan	Methylene blue	530 mg/g	40 °C	(S. Kang et al. 2018)
Carboxymethyl cellulose-chitosan-montmorillonite	Methylene blue	283.9 mg/g	pH 2–10–0 °C to 60 °C	(W. Wang et al. 2020)
Polyacrylamide-g-chitosan	Azo dye	255.5 mg/g	pH 6.0 – 25 °C	(R. C. da silva et al. 2020)
Chitosan-g-poly(acrylic acid)	Methylene blue	1968 mg/g	pH 6.0 – 25 °C	(B. C. Melo et al. 2018)
Chitosan-g-poly (acrylic acid)/vermiculite	Methylene blue	1573.87 mg/g	pH range 2–9/30 °C, 40 °C and 50 °C	(Yi Liu et al. 2010)
Chitosan/starch semi-IPN	Direct red 80 (DR80)	312.77 mg/g	pH 1 to 10–80 °C	(F. A. Ngwabebhoh et al. 2016)
Nano TiO₂/chitosan/poly (N-isopropylacrylamide)	Acid fuchsin (AF)	17.78 mg/g	pH 4.0 – 4 °C	(Jianhua Zhou et al. 2017)
Poly(vinyl-alcohol)-sodium alginate-chitosan montmorillonite	Methylene blue	137.15 mg/g	pH 3 to 10-(20–40 °C)	(W. Wang et al. 2018)
Activated carbon from chitosan coated tea saponin	Methylene blue	604.10 mg/g	pH 6.0 – 30 °C	(Zheng-Wei Ma et al. 2021)
Activated carbon/chitosan/Carica papaya sedes	Methylene blue	302.01 mg/g	pH = 8–30 °C	(E. A. Idohou et al. 2020)
Chitosan–montmorillonite/polyaniline	Methylene blue	111 mg/g	pH = 11–25 °C	(I. M. Minisy et al. 2021)
Chitosan/multiwalled carbon nanotubes	Congo red	450.4 mg/g	pH 5 – 30 °C	(S. Chatterjee et al. 2010)
Chitosan-tripolyphosphate/kaolin clay	Remazol brilliant blue R dye	687.2 mg/g	pH (4–10) – 30 °C	(Jawad and Abdulhameed, 2020)
Bentonite clay, chitosan and acrylic acid	Malachite green Methyl violet	492 mg/g 482 mg/g	pH 7–30 °C	(R. Bhattacharyya, S. K. Ray, 2014)
Chitosan-polyglycidol/coating iron oxide particles	Methylene blue	8.37 mg/g	room temperature	(A. Iovescu et al. 2020)
Chitosan/citric acid modified β-cyclodextrin	Reactive blue 49	498 mg/g	pH 5–25 °C	(J. Zhao et al. 2018)
Triton X-100/chitosan sodium dodecyl sulfate/chitosan	Congo red	378.79 mg/g 318.47 mg/g	pH 5–30 °C	(S. Chatterjee et al. 2009)
Magnetic chitosan/PVA	Congo red	470.1 mg/g	pH 4.0 and 11.0–25 °C	(H.-Y. Zhu et al. 2011).
Chitosan–Fe(III)	Reactive black 5 (RB 5)	349.22 mg/g	pH 7–25 °C	(S. Rashid et al. 2018)
Chitosan/silica/zinc oxide	Methylene blue	293.3 mg/g	pH 7–25 °C	(H. Hassan et al. 2019)
Nano-ZnO/chitosan	Congo Red	120 mg/g	pH 7.0	(Ru Jiang et al. 2021)
Chitosan-glyoxal/ZnO/Fe3O4	Aspergillus niger RB19	363.3 mg/g	pH (4–10) – 60 °C	(A. Reghioua et al. 2021)
2. Hydrogels used for metals removal				
Chitosan-glucose	Co(II)	202 mg/g	pH = 7.0–20 °C	(Y. Liu et al. 2019)
Chitosan/orange peel	Cr(VI) Cu(II)	107.5 mg/g 116.6 mg/g	Cr pH 4.0/Cu pH 5.0 room temperature	(S. Pavithra et al. 2021)
Xanthate-modified chitosan/poly(N-isopropylacrylamide)	Cu(II) Pb(II) Ni(II)	115.1 mg/g 172.0 mg/g 66.9 mg/g	pH 5.0 – 25 °C	(Shuping Wu et al. 2018)
N-quaternized chitosan/poly(acrylic acid)	Cr(III) Fe(III) Ni(II) Cu(II) Cd(II)	275.9 mg/g 599.5 mg/g 398.0 mg/g 503.2 mg/g 1261.7 mg/g	pH 7.4 – 37.5 °C	(R. R. Mohamed et al. 2017)

Table 1 (*continued*)

Adsorbent	Adsorbate	Adsorption capacity (mg/g)	pH - Temperature (°C)	Reference
polydopamine-modified-chitosan	Cr(VI) Pb(II)	374.4 mg/g 441.2 mg/g	pH 5.5 – 25 °C	(D-M. Guo et al. 2018)
β-cyclodextrin/chitosan/ hexamethylenetetramine	Cr(VI)	333.8 mg/g	pH 2 – 25 °C	(Xue-Lian Wang, et al. 2019)
Chitosan -g-methylenebisacrylamide/poly (acrylic acid	Pb(II) Cd(II) Cu(II)	96.62 mg/g 80.57 mg/g 88.94 mg/g	pH 5.5–25 °C	(A. T. Paulino et al. 2011)
Chitosan/acrylicacid/gelatin (semi IPN)	Cu(II)	261.08 mg/g	pH 5.75	(Wen-Bo Wang et al. 2013)
hydroxypropyl chitosan/polyacrylamide/ polyvinyl alcohol	Cr(VI)	102.5641 mg/g	pH 2–25 °C	(Jilong Cao et al. 2021)
poly(vinyl alcohol)-enhanced chitosan hybrids	Cu(II)	38.7 mg/g	pH 4.2 – 25 °C	(Jianming Wu et al. 2019)
1,5-Diphenylcarbazide/chitosan	Cu(II)	185.505 mg/g	pH = 6 – 30 °C	(Mudasir Ahmad et al. 2019)
chitosan/acid-activated montmorillonite	Pb(II) Ni(II)	41.06 mg/g 42.38 mg/g	pH 5.5 – 25 °C	(Ricardo M. Vieira et al. 2018)
Glucan/chitosan	Cu(II) Co(II) Ni(II) Pb(II) Cd(II)	342 mg/g 232 mg/g 184 mg/g 395 mg/g 269 mg/g	pH 7–20 °C	(Chenglong Jiang et al. 2019)
Aluminium-chitosan–Fe(III)	Fl^{-1}	31.16 mg/g	pH 5–25 °C	(J. Ma et al. 2014)
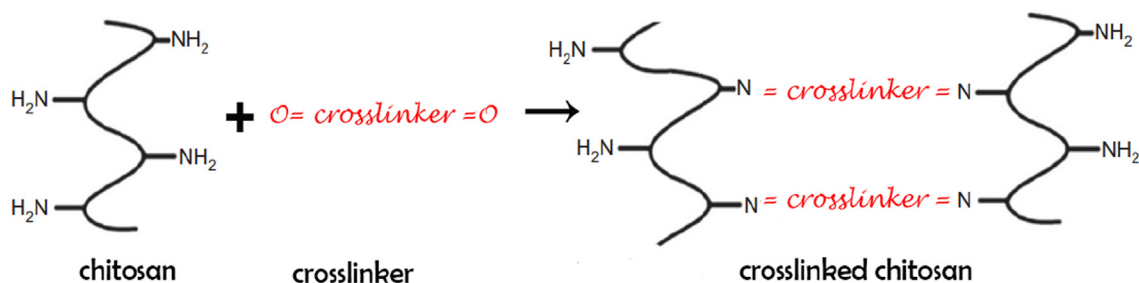
Fig. 2   Formation of crosslinked chitosan.

4. Alginate-based hydrogels to remove metal ions and dyes

Sodium alginate contains this formula and the functions of 1,4-linked -b-D-mannuronic acid and a-L-guluronic acid residues, and it belongs to the natural polymer natural polysaccharide family, as many hydrogels have been prepared from sodium alginate and copolymers with many natural or synthetic materials (such as acrylic acid and acrylamide) forming sodium alginate-based hydrogels. These hydrogels have natural properties, impart mechanical properties and increase the ability to work in all conditions and in all acidic and basic media due to the structure and functional groups of the formed hydrogel, which is useful for creating multitasking systems intended for achieving advanced adsorption properties, gives a wide pH range for the absorption of dyes and metal ions and has stability properties within media, solutions and water, mechanical properties and dissociation resistance properties within solutions due to the formation of hydrogen bonds and charge differences. These properties all lead to improved stability and adsorption behaviour (Bhattacharyya and Ray, 2015; Thakur et al. 2016).

Fig. 4 shows how many types of hydrogels appear and their classification, and Table 2 shows the derived performance for the alginate-based hydrogels.

4.1. Interpenetrating networks (IPNs) and semi-IPNs of alginate

B. Mandal and S. K Ray., successfully synthesized IPN hydrogels using a free radical in situ method with crosslink copolymerization for acrylic acid and hydroxyethyl methacrylate in an aqueous solution of sodium alginate in the presence of N, N-methylenebisacrylamide as a comonomer crosslinker to obtain crosslinked hydrogels to remove congo red and methyl violet from water (Mandal and Ray, 2013). E. S. Dragan and his collaborator obtained cryogels with a full cationic/ionic IPN containing two different opposite charge networks that were crosslink independent. The difference between the preparation of semi-interpenetrating network cryogels and a full IPN is that for the full IPN, one must first add cross-linking polymerization of acrylamide with N,N-methylene bis-acrylamide, and chitosan and then add NaOH with ECH dur-
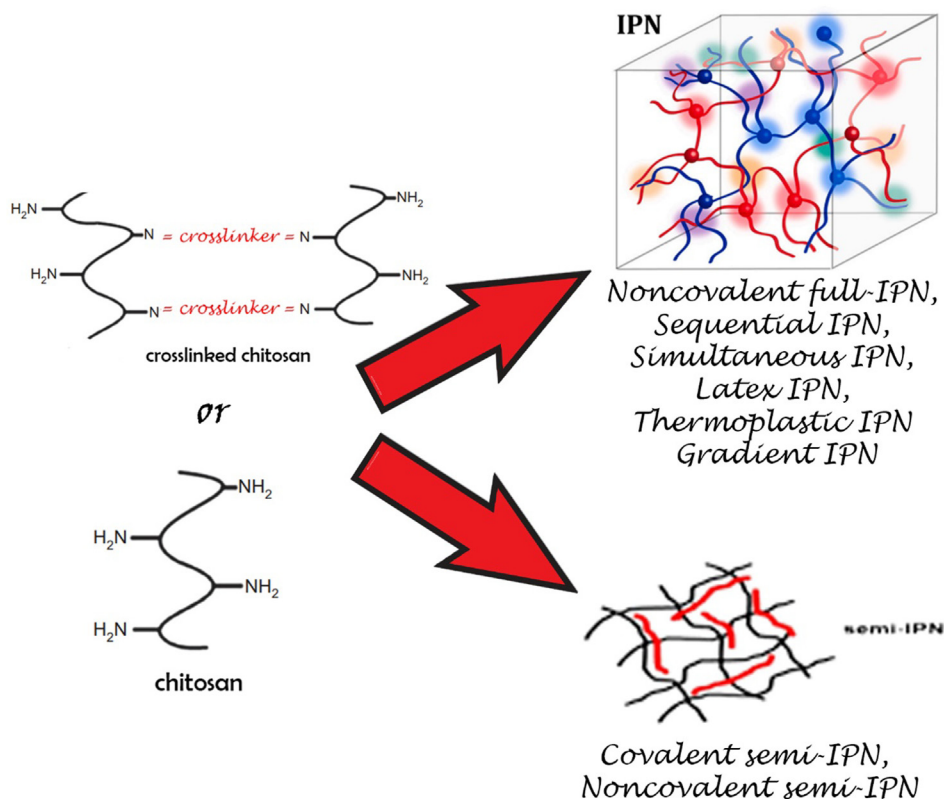
Fig. 3 Formation of the semi-IPN and full-IPN hydrogels starting from chitosan.

ing freezing conditions, as the main big difference between a semi and full IPN is the parameters such as the cross-linker ratio, pH of the chitosan solution, and the chitosan molar mass for the full-IPN as a function of pH and the gel morphology. Additionally, the MB adsorption capacity using the full-IPN cryogel reaches approximately 750 mg/g, which is higher than the adsorption capacity obtained using a semi-IPN (Dragan et al., 2012a; 2012b). Hydrogels were synthesized from sodium alginate, and the copolymer of acrylic acid and acrylamide provided the highest adsorption at almost the highest Q_m (mg/g) due to the structure of acrylamide. The semi-IPN (semi-interpenetrating network) is a crosslinked system with linearly forming hydrogels, and Sharma, A. K and his collaborators in 2019 fabricated semi-IPN nanocomposite hydrogels adsorbents for removal of biebrich scarlet and crystal violet dyes with a maximum adsorption capacity of 100 mg and 500 mg and absorption efficacy of 93.43% and 89.1%, respectively (Sharma et al., 2019).

4.2. Carbon-derived materials incorporated with alginate hydrogels

The fabricated sodium alginate crosslinked acrylic acid/-graphite hydrogel showed unique thermal properties and was used to remove malachite green dye from aqueous solution under the batch adsorption method, showing that the maximum adsorption tendency using the Langmuir model reached 628.93 mg g^{-1} (Verma et al. 2020). Other study shows an acrylamide bonded sodium alginate hydrogel and acrylamide/-graphene oxide bonded sodium alginate nanocomposite hydrogel showed a maximum adsorption capacity of

62.07 mg/g and 100.30 mg/g for crystal violet dye, respectively, as the graphene oxide led to higher adsorption due to its porous structure (Pashaei-Fakhri et al., 2021).

Composite hydrogels were successfully synthesized from modified graphite carbon nitride by a facile cross-linking polymerization method. This improved the adsorption ability of each component to target metal ions and solved the recycling and separation problem of g-C$_3$N$_4$, which is an absorbent powder that is difficult to recycle after adsorption. The maximum absorption capacities for Pb(II), Ni(II), and Cu(II) were calculated to be 383.4 mg/g, 306.3 mg/g, and 168.2 mg/g, respectively (Wei Shen et al. 2020).

4.3. Alginate/synthetic polymer hydrogels

The octaminopropyl polyhedral oligomeric silsesquioxane hydrochloride salt based alginate/polyacrylamide hybrid is a new hydrogel type with mechanical properties suitable for the absorption process and was synthesized using the combination of a double network and POSS nanoparticle DN gels to increase the crosslinking and toughness to show great mechanical properties. DN hydrogels with an increased OA-POSS ratio (N3%), Alg/PAAm/OA-POSS1, show an absorption capacity of more than 20 mg OAAlg/PAAm/OA-POSS1 for methylene blue at pH 9 and 11 (Bahrami et al. 2019).

Another example is sodium alginate polyacrylic acid hydrogel which was synthesized by free radical in situ polymerization to obtain a hydrogel and poly sodium alginate (acrylic acid)/zinc oxide) hydrogel nanocomposite and was used to isolate toxic MB dye from an aqueous solution. A maximum absorption capacity of 1129 mg/g and 1529.6 mg/g was found for the
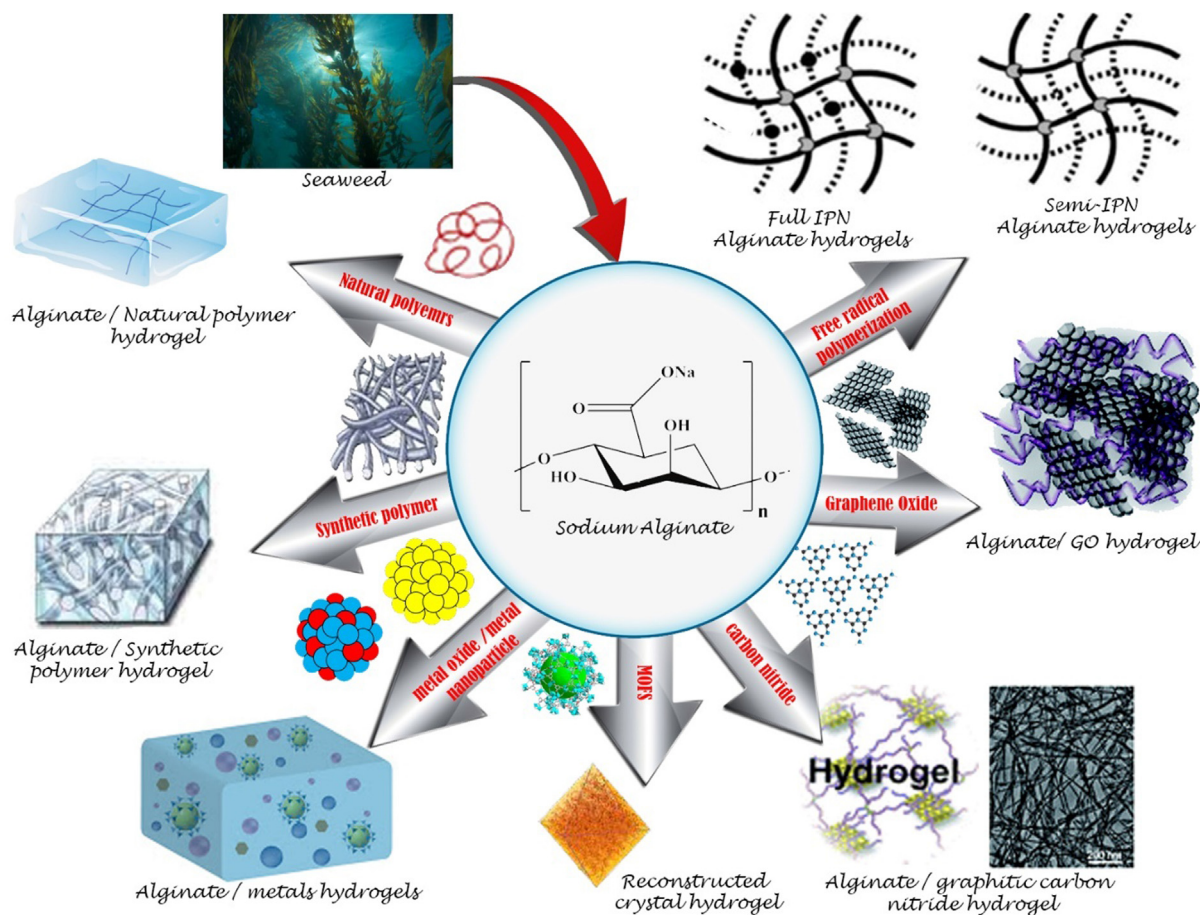
Fig. 4   Sodium alginate hydrogels incorporated with different materials for the adsorption of dyes or metal ions.

sodium alginate polyacrylic acid and poly sodium alginate (acrylic acid)/zinc oxide) hydrogel nanocomposite solution in 0.25 g/L of solution at a pH of 6.0 over 40 min (Makhado et al. 2020).

SA/polyvinyl alcohol/graphene oxide hydrogel microspheres were also prepared in a simple manner. Sodium alginate was physically crosslinked by calcium; GO was encapsulated in the compound to harden the hydrogels; polyvinyl alcohol played an important role in well-dispersed graphene oxide in sodium alginate. The hydrogels were used as an effective adsorbent for removing Cu(II) and U(VI) from aqueous solutions, and the maximum absorption capacities for the hydrogel microspheres for Cu(II) and $UO_2(II)$ were 247.16 mg/g and 403.78 mg/g, respectively (Yi et al. 2018).

In another case, sodium alginate/polyethylene amine compound hydrogel was designed and manufactured to remove heavy metal ions from wastewater. For the absorption of Cu(II) and Pb(II) ions in single and bilateral aqueous solutions and for the absorption of Cu(II) and Cd(II) ions in wastewater, the adsorption capacity was 322.6 mg/g and 344.8 mg/g, respectively. However, in both the alginate and polyethyleneimine segments, in addition to the 3D network structure and a large number of –OH, –COOH and –NH$_2$ groups provide abundant active sites for heavy metal ion absorption (Godiya et al., 2019a; 2019b). Chirag B. Godiya et al. synthesized sodium alginate combined with polyethyleneimine and used it to remove MB in aqueous medium. The sodium algi-

nate/polyethyleneimine hydrogel showed excellent MB removal performance, that is, approximately 99% of dye was removed from water within approximately 30 min with a 0.5 g/L sodium alginate/polyethyleneimine hydrogel at an initial concentration of 100 mg/L. The absorption was carried out by functional groups with chelation between the –NH$_2$, –OH and –COOH groups with MB, with a maximum MB absorption capacity of 400.0 mg/g (Godiya et al., 2020a; Godiya et al., 2020b).

4.4. Alginate incorporated with metals

The microparticles are very small spheres formed by synthesizing calcium alginate microparticles that are small in size and uniformly shaped and obtained using a flow-focusing microfluidic device combined with external gelation in a $CaCl_2$ solution. Due to their size, the microspheres showed efficacy in absorbing Cu(II) and Ni(II) ions from solutions in record time with good heavy metal ion absorption. Since the tiny size of these nanoparticles and within the size of the micro assist in determining the mechanism and evidence established on the exchange of charges and action mechanism between the metal ions from solution, and, therefore the free carboxylic groups of the calcium alginate hydrogels. Where the absorption is bigger, the capacities of the calcium alginate microparticles towards Cu(II) and Ni(II) ions were 0.36 mg/mg and 0.81 mg/mg (Duc et al. 2021).

Table 2 Classification of alginate-based hydrogels and their adsorption conditions and performances.

Adsorbent	Adsorbate	Adsorption capacity (mg/g)	pH - Temperature (°C)	Reference
1. Hydrogels used for dyes removal				
Oxide-montmorillonite/sodium alginate	Methylene blue	150.66 mg/g	pH 5.99–30 °C	(Tao et al., 2020)
Magnetic/β-cyclodextrin/activated charcoal/Na alginate	Methyl violet Brilliant green	5.882 mg/g 2.283 mg/g	pH 6- 35 °C − 55 °C	(S. Yadav et al. 2021)
Alginate- cobalt ferrite	Reactive red 195 Reactive yellow 145	106.75 mg/g 75.95 mg/g	pH 6- 25 – 45 °C	(R. Jayalakshmi and Jeyanthi, 2021)
Sodium alginate poly(acrylic acid)/zinc oxide	Methylene blue	1129 mg/g 1529.6 mg/g	pH 6–25 °C	(Edwin Makhado et al. 2020)
Sodium alginate/polyethyleneimine	Methylene blue	400.0 mg/g	pH 5.5–25 °C	(Chirag B. Godiya et al. 2020)
Oxidized alginate/gelatin decorated silver	Methylene blue	625 mg/g	pH 7- 30 °C	(Ragab E. Abou-Zeid et al. 2019)
Alginate/carboxymethyl cellulose/TiO$_2$	Methylene blue Malachite green	600–700 mg/g 300–350 mg/g	pH 7.0- 25 °C	(Young Sil Jeon et al. 2008)
2. Hydrogels used for metals removal				
Graphene oxide/alginate	Cr(III) Pb(II)	118.6 mg/g 327.9 mg/g	pH $_{Cr}$ 6.0 – 25 °C pH $_{Pb}$ 5.0 – 25 °C	(Chengling Bai et al. 2020)
Amino-carbamate moiety -g- calcium alginate	Ag(I)	210 mg/g	25 °C- pH 5.0	(Hamza Shehzad et al. 2020).
3D network nanostructured sodium alginate	Cd(II) Cu(II)	9.54 mg/g 13.38 mg/g	pH $_{Cd}$ = 7–30 °C pH $_{Cu}$ = 6	(Xiaojun Tao et al. 2021)
alginate/polyethyleneimine	Cu(II) Pb(II) Cu(II) Pb(II)	322.6 mg/g 344.8 mg/g 128.2 mg/g 138.9 mg/g	pH 5.5–25 °C	(C. B. Godiya et al. 2019)
Crosslinked chitosan/sodium alginate/calcium ion	Pb(II) Cu(II) Cd(II)	176.50 mg/g 70.83 mg/g 81.25 mg/g	25 °C	(Shuxian Tang et al. 2020)
Sodium alginate grafted polyacrylamide/graphene oxide	Cu(II) Pb(II)	68.76 mg/g 240.69 mg/g	pH $_{Cu}$ = 5– 25 °C PH $_{pb}$ = 5.5	(Huabin Jiang et al. 2020)
Alginate modified graphitic carbon nitride	Pb(II) Ni(II) Cu(II)	383.4 mg/g 306.3 mg/g 168.2 mg/g	20 °C pH = 6	(Wei Shen et al. 2020)
Sodium alginate/polyvinyl alcohol/graphene oxide	Cu(II) UO$_2$ (II)	247.16 mg/g 403.78 mg/g	pH: 4.0–4.5– 25 °C	(Xiaofeng Yi et al. 2018)
Thermoresponsive alginate/starch ether	Cu(II)	25.81 mg/g	pH 5.5–20 °C	(Mingyun Dai et al. 2019)
Alginate - Cobalt ferrite	Cu(II) Cr(VI)	169.5 mg/g 72.5 mg/g		(Sourbh Thakur et al. 2019)

4.5. Alginate/natural polymer hydrogel

A heat responsive (thermoresponsive) hydrogel containing sodium alginate and 2-hydroxy-3 isopropoxypropyl starch was developed to remove Cu(II) from an aqueous solution. The hydrogel showed a lattice and porous structure, as well as abundance of carboxyl groups within the structure, giving it sufficient binding sites for Cu(II) absorption, and the maximum absorption capacity was 25.81 mg/g. In addition, the hydrogel could be successfully absorbed with only small amounts of dilute HCl within a short period of time due its heat-responsive property, and it also showed the feasibility of regeneration, because the adsorption capacity of Cu (II) remained higher than 15.23 ± 0.27 mg/g even after five cycles. For example, the absorption capacities of the hydrogel gel beads and sodium at pH 4.5 were 22.37 ± 0.18 mg/g and 15.01 ± 0.21 mg/g, respectively (Dai et al. 2019).

4.6. Sodium alginate hydrogel membranes

4.6.1. Sodium alginate cross-linked membranes
Membranes with natural properties have been prepared from available materials and form an environmentally friendly polymer that is useful for removing contamination of organic dye by calcium alginate, which forms a stable gel structure by molecular chains of sodium alginate interconnected by chelating formation with calcium ions, and minute voids are formed by olethylene glycol (OEG) or polyethylene glycol (PEG) is added to the casting polymer solution and OEG or PEG is then removed from the membranes by a washing process after

cross-linking. Promising filtration membranes for removing organic dyes from water resources have been successfully prepared from calcium alginate and cross-linked by chelating formation with calcium ions called Egg-Box Junction (Kashima et al., 2021).

4.6.2. Nanofiltration membranes

Nanofiltration membranes were successfully fabricated and the PVAGO-NaAlg nanocomposite hydrogel was formed by mixing with the phase inversion caused by the immersion deposition technique. Wetting and modified PES membranes containing 1 wt% HG showed higher rejection of BSA solution and compared with PES and PES/1 wt% PVP films. The rejection of BSA solution of membranes with 5% wt HG added 97.36% was reported and that it can be described These increases as slight increases in rejection of BSA solution, and any increase in the amount of HG added adds associated with the resistance of PES films and improvement in the antifouling ability with results of 84.22, 86.2, 88.1, 88.9% For membrane modified 1 wt% PVP 0.5, 1, 2 and 5% by weight HG, respectively.

The interaction between the dye functional groups and the functional groups on the surface of the hydrogel-blended membranes which prevents passage through the membranes, causes negative charge on the membranes surface and promotes the dye's rejection of the membranes through hydrogen bonding or π-π stacking interactions to the adsorption of dye molecules (Amiri et al., 2020).

4.6.3. Double-crosslinked nanofiltration membrane

Alginate films were made and these films are based on graphene oxide (GO) by stacking graphene oxide nanolayers and have the ability to separate dye from water. A double crosslinked graphene oxide compound (Ca/GO-SAx) was made by adding sodium alginate (SA) and calcium ions are attached to the porosity and make the nano-channel useful for de-dyeing achieves the removal of more than 99% of the multiple dyes (Congo red, crystal violet, methylene blue) and excellent dye separation performance for methyl blue, congo red, crystal violet and direct red 80. The removal capacity to the water flow is of the order of 38.90 L m-2h1bar-1 which is due to the 384% increase of the GO membrane alone and because the alginate makes the structure of the Ca/GO-SA3 complex membrane more compact, organized and constant interlayer spacing in brine solutions. It is highly stable in water or even strong acid and alkaline solutions (Yu et al., 2021).

4.7. Hydrogels as photocatalyst functionalization

4.7.1. Sodium alginate hydrogel as film

The alginate hydrogels based on alginate supported with Ag2O hydrogel film (Ag2O/sodium alginate supramolecular hydrogel film) by using the solution casting method photodegradation as the alginate can react with Ag + thru fast synthesis form SMH film and in water form Ag2O in situ and the results rates were above 93% for both dyes Methylene blue and Malachite green. Hypothetically, the reusability of the current hydrogel depends (electron donors) under light irradiation by reducing lattice Ag+ and the effective reusability reach 90% (Ma et al. 2017).

4.7.2. Photocatalytic alginate hydrogel beads

Developing poly(vinyl alcohol) (PVA)/sodium alginate (SA) hydrogel beads using FeCl3 and boric acid as cross-linking agents and by degradation of tetracycline (TC) under visible-light irradiation to form PVA/SA-FeCl3 beads as reusable and durable photo-Fenton performance catalyst and shows great importance for the practical application in the environmental remediation with a removal rate of TC reaches 90.5% and mineralization efficiency removal of organic carbon reaches 28.6% under optimized conditions after 60 min irradiation under visible-light irradiation. The improvement can exhibit good cyclic stability and the photo-Fenton catalytic activity (Du et al., 2021).

4.8. MOF-incorporated Cu-based alginate/PVA hydrogel

(MOF)-incorporated single-network alginate (MOF-Alg(Cu)) beads were used to adsorb ions in seawater. MOF-incorporated Cu-based alginate/PVA hydrogel (MOF-Alg(Cu)/PVA) beads were fabricated to enhance the ion adsorption desalination technique. Cu-based MOFs were successfully synthesized in situ on an interpenetrating polymer network (IPN). Given that the IPN hydrogel beads have high stability, the amount of MOF particles extracted during the adsorption of ions is reduced as the concentration of seawater is reduced to 1500 ppm at stage six with an ion removal efficiency of 95.7% (Lee et al. 2021).

5. Chitosan/Alginate compound hydrogel

1. Chitosan / Alginate with activated carbon hydrogel

The use of alginate with chitosan to combine activated carbon (AC) is widely known in water treatment, where natural polymers were added to overcome the technical problems that carbon suffers from, such as its high cost and difficulty in recovering it, as well as the alternating current particles were encapsulated, and this packaging results in compounds with superior mechanical properties, low cost, and a greater number of functional groups (Quesada et al., 2020)

2. Crosslinking Chitosan / Alginate hydrogels

The gel nanoparticles were formed containing Chitosan and alginate by ionic cross-linking with sodium tripolyphosphate and the equilibrium adsorption capacity of Cu2 + particles was explored from copper sulfate solutions at constant pH. The Adsorption occurs in copper sulfate solution Low concentration (0.5–50 mM) and highly concentrated (50 mM to 1 M) solution (Yu et al., 2013)

3. Alginate–chitosan hybrid gel

Alginic and chitosan as one of the most effective adsorbents for removing heavy metal ions from the waste water stream to the simultaneous use of alginic acid and chitosan, which is expected to form carboxyl groups on alginic acid and amino groups on chitosan and the cross-linking reaction made the beads durable under acidic conditions. The adsorption of Cu (II), Co(II) and Cd(II) onto the beads was significantly rapid

and reached equilibrium within 10 min at 25 °C and the adsorption was about 70 mg/g (Gotoh et al., 2004).

4. Clay / Chitosan / Alginate hydrogels Magnetic functionalization

Chitosan/Alginate Hydrogel beads compounds based on magnetic bentonite/carboxymethyl chitosan/sodium alginate (Mag-Ben/CCS/Alg) and has ability to absorb copper ions in water to equilibrium after 90 min of adsorption and copper (II) removal ability 92.62%, and the maximum adsorption capacity is 56.79 mg/g (30 °C) above 80% after recycling four times and the qmax reached 56.79 mg/g (30 °C) and the Cu(II) adsorption is spontaneous and endothermic process and rather It also has the magnetic properties of Fe3O4. It can easily achieve liquid–solid separation after adsorption (Zhang et al., 2019).

6. Adsorption and depollution mechanism

The depollution processes are Adsorption techniques, photocatalytic, membrane processes, Magnetic separation processes.

There are several proposed mechanisms such as electron acceptor (EDA) in interactions, hydrophobic interactions, hydrogen bonding, and dipole force, as possible explanations for the harmful adsorption of organic compounds (see Fig. 5).

The π electron-rich on the surface played a role in addition to the porosity of the absorbent material and beside the thermal decomposition begins with the homogeneous decomposition of the C-C bond next to the carboxyl group (Sasi et al., 2021).

Where heavy metals are absorbed by ion exchange adsorption filtration reverse osmosis flocculation / sedimentation and while dyes deteriorate filtration adsorption.

Activated carbon is characterized as a material with a highly porous carbon internal structure obtained from pyrolysis and chemical processing and is suitable for the adsorption of organic compounds, especially pollutants with aromatic functions. Adsorption is largely carried out through π interactions between the adsorbent and the AC surface as well as through hydrogen bonding and cation/anion interactions with metal species from van der Waals (Sweetman et al., 2017).

Where it was found that at low pH values the presence of H + ions and by enhancing the surface of the protons of func-

tional groups such as carboxyl, amide and hydroxyl groups, more of these positive charges can be obtained, and the absorption can be controlled by obtaining a certain pH (Steinegger et al., 2020; Kord Forooshani and Lee, 2017).

Magnetic separation is a common method for water purification, which can be from oil removal, removal of inorganic and organic ions, based on adsorption, catalytic processes, or membrane processes. In addition, magnetic components can help improvise the separation efficiency.

Magnetism as it has a unique physical property by affecting the physical properties of pollutants in water and where magnetic separation provides a popular adoption of water purification technology (see Fig. 6).

Photocatalysis is defined as the acceleration of photochemical transformation by a metal oxide catalyst such as TiO2 or Fenton reagent. The most widely used catalyst for all photocatalytic studies is known and the most common is rutile TiO2. Photocatalysis is known to be the most suitable process for organic and effluents containing a high percentage of COD (chemical oxygen demand) and for the complete conversion of highly heat-resistant organic pollutants to reach the level of biological treatment (Gadipelly et al. 2014).

The semiconductors are popular and used as effective photocatalysts such as (TiO_2, ZnO, SnO_2, $SrTiO_3$, Fe_2O_3, etc.), the photocatalytic reaction adopts the main types such as holes (h +), hydroxyl radicals (OH) and superoxide radicals (O_2^-) (Alakhras et al. 2020).

Where the periodic table was independently developed by Dmitri Mendeleev in Russia (1869) and Lothar Mayer in Germany (1870) and it was approved that there is a periodic relationship between the properties of the elements known at that time and was developed with time. It was noted that there is a difference between the elements significantly in their chemical and physical properties, but also there are some elements similar in their behaviours.

Other elements are not shiny, malleable or ductile, and they are poor conductors of heat and electricity. These properties, in addition to the atomic diameter, affect the absorption difference in hydrogels. We can sort the elements into large classes with common properties.

Metals (shiny, malleable elements, good conductors of heat and electricity - highlighted in yellow); nonmetals (elements that appear faint, poor conductors of heat and electricity - highlighted in green); and metalloids (elements that conduct
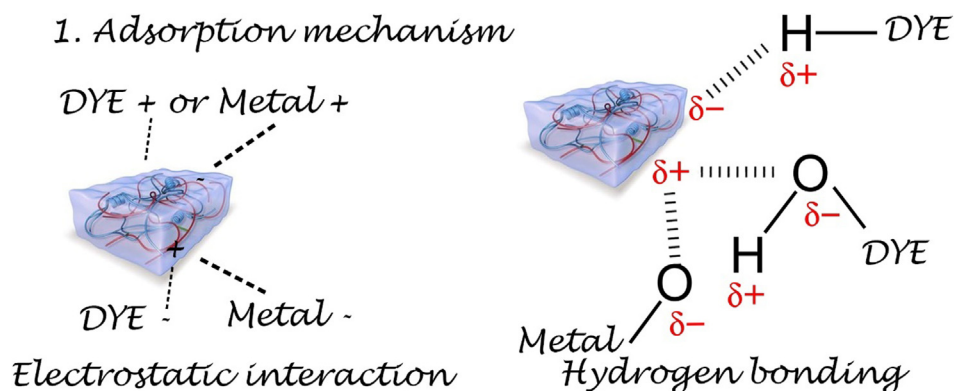
Fig. 5 Scheme of dye or metal ion adsorption on biobased hydrogel.
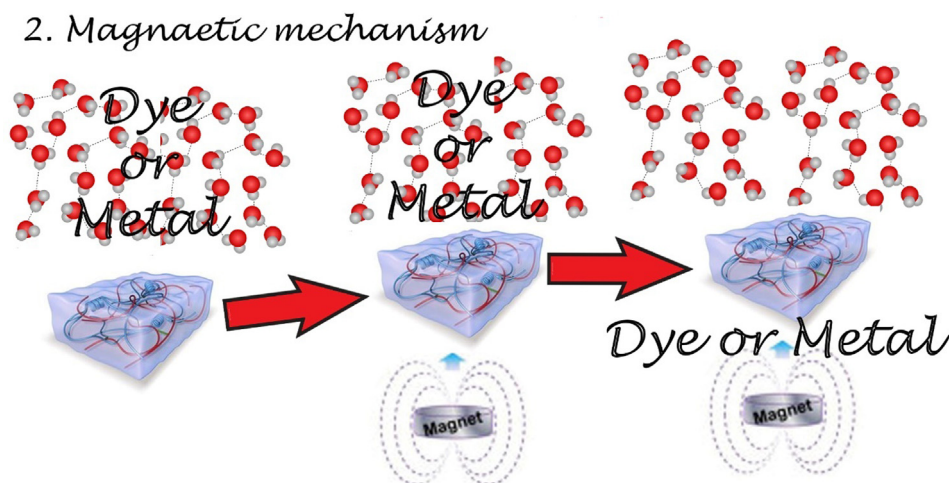
Fig. 6   Scheme of magnetic separation of dyes or metal ions.

heat and electricity fairly well, have some properties of metals and some properties of nonmetals - shaded magenta) (Brown et al., 2018).

7. Perspectives and conclusions

Studies have shown that chemically polluted water often contains heavy metals and causes serious environmental problems such as possible human poisoning. Additionally, chemical pollution often contains pollutants in the form of liquid wastes from textiles, factories, water desalination centres, etc. This produces very polluted waste with a high concentration of chemical and biochemical oxygen demand and a large amount of suspended and colloidal solids, salts, heavy metals, and other solid or nondegradable organic matter, which poses a significant threat to the environment when drainage parameters are not accurate. In recent times, the use of adsorption technology based on natural polymers originating as polysaccharides and biobased polymers that are considered to be of high abundance in nature has been a promising alternative, and has been proven to be able to remove heavy metal pollutants and liquid wastes. Appropriate results have been achieved in removing many water pollutants, such as traditional, widespread and highly effective materials. Adsorption is recognized as one of the most well-known and effective technique for removing water pollution because it is an efficient, cost-effective, and environmentally friendly treatment method. Hydrogels based on chitosan and alginate are considered promising materials for removing heavy metals and liquid wastes from textiles and other pollutants, and they depend on reaction mechanisms such as electrostatic attraction and chelating gels to improve the adsorption properties of many pollutants; inorganic and organic aqueous solutions can be laden with nanomaterial hydrogels. Additionally, hydrogels might be loaded and incorporated with carbon nanomaterials; they are also effective in eliminating various water pollutants, and magnetic biobased hydrogels have the added benefit of magnetic separation and regeneration of absorbents. Several new functional hydrogels have shown excellent absorption capacity for dyes and heavy metals, with peak absorption and selectivity for

porous materials. Table 1 shows that the chitosan-g-poly (acrylic acid) and chitosan-g-poly(acrylic acid)vermiculite hydrogels have the highest dye absorption values for methylene blue dye, with maximum absorption capacities of 1968 mg/g and 1573.87 mg/g, respectively, which is due to electrostatic interactions between the carboxylate groups – COO^- and the methylene blue dye. Creating grafted polymer hydrogels and polymer/clay hydrogels with low-cost properties and high adsorption, as well a N-quaternized chitosan/ poly(acrylic acid) hydrogel, showed high adsorption for Fe (III), Ni(II), Cu(II), Cd(II) metal ions with a maximum adsorption capacity of 599.5 mg/g, 398.0 mg/g, 503.2 mg/g, 1261.7 mg/g, respectively. Polydopamine-modified-chitosan showed high adsorption for heavy metals with a maximum adsorption capacity of 374.4 mg/g and 441.2 mg/g for Cr (VI) and Pb(II), respectively. Table 1 shows the importance of studying and fabricating chitosan hydrogels for water treatment. Sodium alginate poly(acrylic acid) and sodium alginate poly(acrylic acid)/zinc oxide have the highest adsorption capacity for methylene blue dye, with adsorption capacities of 1129 mg/g 1529.6 mg/g, and sodium alginate / polyethyleneimine has the highest adsorption capacity for heavy metals, with an adsorption capacity of 322.6 mg/g and 344.8 mg/g for Cu(II) and Pb(II), respectively. These results show the ability of alginate hydrogels and their effectiveness towards absorption.

Finally, chitosan and alginate represent an abundant, bioavailable, biodegradable, and eco sustainable materials both can be modified physically or chemically to obtain adsorbents of dyes and metal ions. The compositional diversity, and the functional groups confer active adsorption binding sites and reactivity for possible chemical modifications and/or combination with different chemical compounds and/or materials with the aim of increasing the adsorption capacity and efficiency of the adsorbents. The adsorption performance was mainly dependent on the structure, chemical composition, and morphology of the adsorbent as well as environmental variables, such as temperature, pH, and ionic strength. For this reason, the continuity of research is important and the development of innovative materials from biopolymers should continue in the near future.

Acknowledgements

References

Amiri, S., Asghari, A., Vatanpour, V., Rajabi, M., 2020. Fabrication and characterization of a novel polyvinyl alcohol-graphene oxide-sodium alginate nanocomposite hydrogel blended PES nanofiltration membrane for improved water purification. Sep. Purif. Technol. 250, 117216.

Ahmad, M., Zhang, B., Wang, J., Xu, J., Manzoor, K., Ahmad, S., Ikram, S., 2019. New method for hydrogel synthesis from diphenylcarbazide chitosan for selective copper removal. Int. J. Biol. Macromol. 136, 189–198.

Abou-Zeid, R.E., Awwad, N.S., Nabil, S., Salama, A., Youssef, M. A., 2019. Oxidized alginate/gelatin decorated silver nanoparticles as new nanocomposite for dye adsorption. Int. J. Biol. Macromol. 141, 1280–1286.

Akter, M., Bhattacharjee, M., Dhar, A.K., Rahman, F.B.A., Haque, S., Rashid, T.U., Kabir, S.M., 2021. Cellulose-based hydrogels for wastewater treatment: a concise review. Gels 7 (1), 30.

Alakhras, F., Alhajri, E., Haounati, R., Ouachtak, H., Addi, A.A., Saleh, T.A., 2020. A comparative study of photocatalytic degradation of Rhodamine B using natural-based zeolite composites. Surf. Interfaces 20, 100611.

Bahrami, Z., Akbari, A., Eftekhari-Sis, B., 2019. Double network hydrogel of sodium alginate/polyacrylamide cross-linked with POSS: Swelling, dye removal and mechanical properties. Int. J. Biol. Macromol. 129, 187–197.

Bai, C., Wang, L., Zhu, Z., 2020. Adsorption of Cr (III) and Pb (II) by graphene oxide/alginate hydrogel membrane: Characterization, adsorption kinetics, isotherm and thermodynamics studies. Int. J. Biol. Macromol. 147, 898–910.

Bashir, S., Hina, M., Iqbal, J., Rajpar, A.H., Mujtaba, M.A., Alghamdi, N.A., Wageh, S., Ramesh, K., Ramesh, S., 2020. Fundamental concepts of hydrogels: synthesis, properties, and their applications. Polymers 12 (11), 2702.

Bhattacharyya, R., Ray, S.K., 2014. Micro-and nano-sized bentonite filled composite superabsorbents of chitosan and acrylic copolymer for removal of synthetic dyes from water. Appl. Clay Sci. 101, 510–520.

Bhattacharyya, R., Ray, S.K., 2015. Adsorption of industrial dyes by semi-IPN hydrogels of acrylic copolymers and sodium alginate. J. Ind. Eng. Chem. 22, 92–102.

Bolisetty, S., Peydayesh, M., Mezzenga, R., 2019. Sustainable technologies for water purification from heavy metals: review and analysis. Chem. Soc. Rev. 48 (2), 463–487.

Brown, T. E., LeMay, H. E., Bursten, B. E., Murphy, C. J., Woodward, P. M. & Stoltzfus, M. E., 2018, 14 ed. Pearson. 1428 p.

Cao, J., He, G., Ning, X., Wang, C., Fan, L., Yin, Y., Cai, W., 2021. Hydroxypropyl chitosan-based dual self-healing hydrogel for adsorption of chromium ions. Int. J. Biol. Macromol. 174, 89–100.

Chang, Z., Chen, Y., Tang, S., Yang, J., Chen, Y., Chen, S., Li, P., Yang, Z., 2020. Construction of chitosan/polyacrylate/graphene oxide composite physical hydrogel by semi-dissolution/acidification/sol-gel transition method and its simultaneous cationic and anionic dye adsorption properties. Carbohydr. Polym. 229, 115431.

Chatterjee, S., Lee, M.W., Woo, S.H., 2010. Adsorption of congo red by chitosan hydrogel beads impregnated with carbon nanotubes. Bioresour. Technol. 101 (6), 1800–1806.

Chatterjee, S., Lee, D.S., Lee, M.W., Woo, S.H., 2009. Congo red adsorption from aqueous solutions by using chitosan hydrogel beads impregnated with nonionic or anionic surfactant. Bioresour. Technol. 100 (17), 3862–3868.

Roy Choudhury, A.K., 2014. In: Environmental impacts of the textile industry and its assessment through life cycle assessment. Springer, Singapore, pp. 1–39.

Clark, M. ed., 2011. Handbook of textile and industrial dyeing: principles, processes and types of dyes. Elsevier.

Crini, G., 2005. Recent developments in polysaccharide-based materials used as adsorbents in wastewater treatment. Prog. Polym. Sci. 30 (1), 38–70.

Cui, L., Jia, J., Guo, Y., Liu, Y., Zhu, P., 2014. Preparation and characterization of IPN hydrogels composed of chitosan and gelatin cross-linked by genipin. Carbohydr. Polym. 99, 31–38.

da Silva, R.C., de Aguiar, S.B., da Cunha, P.L.R., de Paula, R.C.M., Feitosa, J.P.A., 2020. Effect of microwave on the synthesis of polyacrylamide-g-chitosan gel for azo dye removal. React. Funct. Polym. 148, 104491.

Dai, M., Liu, Y., Ju, B., Tian, Y., 2019. Preparation of thermoresponsive alginate/starch ether composite hydrogel and its application to the removal of Cu (II) from aqueous solution. Bioresour. Technol. 294, 122192.

De Gisi, S., Lofrano, G., Grassi, M., Notarnicola, M., 2016. Characteristics and adsorption capacities of low-cost sorbents for wastewater treatment: a review. Sustain. Mater. Technol. 9, 10–40.

Dragan, E.S., Perju, M.M., Dinu, M.V., 2012a. Preparation and characterization of IPN composite hydrogels based on polyacrylamide and chitosan and their interaction with ionic dyes. Carbohydr. Polym. 88 (1), 270–281.

Dragan, E.S., Lazar, M.M., Dinu, M.V., Doroftei, F., 2012b. Macroporous composite IPN hydrogels based on poly (acrylamide) and chitosan with tuned swelling and sorption of cationic dyes. Chem. Eng. J. 204, 198–209.

Du, Z., Liu, F., Xiao, C., Dan, Y., Jiang, L., 2021. Fabrication of poly (vinyl alcohol)/sodium alginate hydrogel beads and its application in photo-Fenton degradation of tetracycline. J. Mater. Sci. 56 (1), 913–926.

Duc, T.H., Vu, T.K., Dang, C.T., La, D.D., Kim, G.M., Chang, S. W., Bui, X.T., Dang, T.D., Nguyen, D.D., 2021. Synthesis and application of hydrogel calcium alginate microparticles as a biomaterial to remove heavy metals from aqueous media. Environ. Technol. Innovation 22, 101400.

Gadipelly, C., Pérez-González, A., Yadav, G.D., Ortiz, I., Ibáñez, R., Rathod, V.K., Marathe, K.V., 2014. Pharmaceutical industry wastewater: review of the technologies for water treatment and reuse. Ind. Eng. Chem. Res. 53 (29), 11571–11592.

Gotoh, T., Matsushima, K., Kikuchi, K.I., 2004. Preparation of alginate–chitosan hybrid gel beads and adsorption of divalent metal ions. Chemosphere 55 (1), 135–140.

Godiya, C.B., Ruotolo, L.A.M., Cai, W., 2020a. Functional biobased hydrogels for the removal of aqueous hazardous pollutants: current status, challenges, and future perspectives. J. Mater. Chem. A 8 (41), 21585–21612.

Godiya, C.B., Cheng, X., Deng, G., Li, D., Lu, X., 2019a. Silk fibroin/polyethylenimine functional hydrogel for metal ion adsorption and upcycling utilization. J. Environ. Chem. Eng. 7, (1) 102806.

Godiya, C.B., Liang, M., Sayed, S.M., Li, D., Lu, X., 2019b. Novel alginate/polyethyleneimine hydrogel adsorbent for cascaded removal and utilization of Cu2+ and Pb2+ ions. J. Environ. Manage. 232, 829–841.

Godiya, C.B., Xiao, Y., Lu, X., 2020b. Amine functionalized sodium alginate hydrogel for efficient and rapid removal of methyl blue in water. Int. J. Biol. Macromol. 144, 671–681.

Guo, D.M., An, Q.D., Xiao, Z.Y., Zhai, S.R., Yang, D.J., 2018. Efficient removal of Pb (II), Cr (VI) and organic dyes by polydopamine modified chitosan aerogels. Carbohydr. Polym. 202, 306–314.

Ibrahim, N.A., Nada, A.A., Eid, B.M., 2018. Polysaccharide-based polymer gels and their potential applications. In: Polymer Gels. Springer, Singapore, pp. 97–126.

Idohou, E.A., Fatombi, J.K., Osseni, S.A., Agani, I., Neumeyer, D., Verelst, M., Mauricot, R., Aminou, T., 2020. Preparation of activated carbon/chitosan/Carica papaya seeds composite for efficient adsorption of cationic dye from aqueous solution. Surf. Interfaces 21, 100741.

Iovescu, A., Stîngă, G., Maxim, M.E., Gosecka, M., Basinska, T., Slomkowski, S., Angelescu, D., Petrescu, S., Stănică, N., Băran, A., Anghel, D.F., 2020. Chitosan-polyglycidol complexes to coating iron oxide particles for dye adsorption. Carbohydr. Polym. 246, 116571.

Jayalakshmi, R., Jeyanthi, J., 2021. Dynamic modelling of Alginate-Cobalt ferrite nanocomposite for removal of binary dyes from textile effluent. J. Environ. Chem. Eng. 9, (1) 104924.

Jamali, M., Akbari, A., 2021. Facile fabrication of magnetic chitosan hydrogel beads and modified by interfacial polymerization method and study of adsorption of cationic/anionic dyes from aqueous solution. J. Environ. Chem. Eng. 9, (3) 105175.

Jawad, A.H., Abdulhameed, A.S., 2020. Facile synthesis of cross-linked chitosan-tripolyphosphate/kaolin clay composite for decolourization and COD reduction of remazol brilliant blue R dye: optimization by using response surface methodology. Colloids Surf., A 605, 125329.

Jeon, Y.S., Lei, J., Kim, J.H., 2008. Dye adsorption characteristics of alginate/polyaspartate hydrogels. J. Ind. Eng. Chem. 14 (6), 726–731.

Jiang, R., Zhu, H.Y., Fu, Y.Q., Jiang, S.T., Zong, E.M., Zhu, J.Q., Zhu, Y.Y., Chen, L.F., 2021. Colloidal CdS sensitized nano-ZnO/chitosan hydrogel with fast and efficient photocatalytic removal of congo red under solar light irradiation. Int. J. Biol. Macromol. 174, 52–60.

Jiang, H., Yang, Y., Lin, Z., Zhao, B., Wang, J., Xie, J., Zhang, A., 2020. Preparation of a novel bio-adsorbent of sodium alginate grafted polyacrylamide/graphene oxide hydrogel for the adsorption of heavy metal ion. Sci. Total Environ. 744, 140653.

Jiang, C., Wang, X., Wang, G., Hao, C., Li, X., Li, T., 2019. Adsorption performance of a polysaccharide composite hydrogel based on crosslinked glucan/chitosan for heavy metal ions. Compos. B Eng. 169, 45–54.

Kashima, K., Inage, T., Yamaguchi, Y., Imai, M., 2021. Tailorable regulation of mass transfer channel in environmentally friendly calcium alginate membrane for dye removal. J. Environ. Chem. Eng. 9, (3) 105210.

Kang, S., Zhao, Y., Wang, W., Zhang, T., Chen, T., Yi, H., Rao, F., Song, S., 2018. Removal of methylene blue from water with montmorillonite nanosheets/chitosan hydrogels as adsorbent. Appl. Surf. Sci. 448, 203–211.

Kaur, A., Jindal, R., 2019. Comparative study on the behaviour of Chitosan-Gelatin based Hydrogel and nanocomposite ion exchanger synthesized under microwave conditions towards photocatalytic removal of cationic dyes. Carbohydr. Polym. 207, 398–410.

Kia, A., Rastegary, M., Dara, A., Banki, M.S., Rezaei, E., Ebrahimi, F., Alizade, M., 2017. Experimental study of Siri-Island refinery wastewater treatment using a photocatalytic process. Energy Sources Part A 39 (2), 232–239.

Kord Forooshani, P., Lee, B.P., 2017. Recent approaches in designing bioadhesive materials inspired by mussel adhesive protein. J. Polym. Sci., Part A: Polym. Chem. 55 (1), 9–33.

Lee et al, 2021. Adsorptive seawater desalination using MOF-incorporated Cu-alginate/PVA beads: Ion removal efficiency and durability. Chemosphere 268, 128797.

Liu, Y., Hu, L., Yao, Y., Su, Z., Hu, S., 2019. Construction of composite chitosan-glucose hydrogel for adsorption of Co2+ ions. Int. J. Biol. Macromol. 139, 213–220.

Liu, Y., Huang, S., Zhao, X., Zhang, Y., 2018. Fabrication of three-dimensional porous β-cyclodextrin/chitosan functionalized graphene oxide hydrogel for methylene blue removal from aqueous solution. Colloids Surf., A 539, 1–10.

Liu, Y., Zheng, Y., Wang, A., 2010. Enhanced adsorption of Methylene Blue from aqueous solution by chitosan-g-poly (acrylic acid)/vermiculite hydrogel composites. J. Environ. Sci. 22 (4), 486–493.

Ma, Y., Wang, J., Xu, S., Zheng, Z., Du, J., Feng, S., Wang, J., 2017. Ag 2 O/sodium alginate supramolecular hydrogel as a film photocatalyst for removal of organic dyes in wastewater. RSC Adv. 7 (25), 15077–15083.

Ma, Z.W., Zhang, K.N., Zou, Z.J., Lü, Q.F., 2021. High specific area activated carbon derived from chitosan hydrogel coated tea saponin: One-step preparation and efficient removal of methylene blue. J. Environ. Chem. Eng. 9, (3) 105251.

Ma, J., Shen, Y., Shen, C., Wen, Y., Liu, W., 2014. Al-doping chitosan–Fe (III) hydrogel for the removal of fluoride from aqueous solutions. Chem. Eng. J. 248, 98–106.

Makhado, E., Pandey, S., Modibane, K.D., Kang, M., Hato, M.J., 2020. Sequestration of methylene blue dye using sodium alginate poly (acrylic acid)@ ZnO hydrogel nanocomposite: kinetic, isotherm, and thermodynamic investigations. Int. J. Biol. Macromol. 162, 60–73.

Mandal, B., Ray, S.K., 2013. Synthesis of interpenetrating network hydrogel from poly (acrylic acid-co-hydroxyethyl methacrylate) and sodium alginate: modeling and kinetics study for removal of synthetic dyes from water. Carbohydr. Polym. 98 (1), 257–269.

Maity, J., Ray, S.K., 2014. Enhanced adsorption of methyl violet and congo red by using semi and full IPN of polymethacrylic acid and chitosan. Carbohydr. Polym. 104, 8–16.

Mahmoud, G.A., Sayed, A., Thabit, M., Safwat, G., 2020. Chitosan biopolymer based nanocomposite hydrogels for removal of methylene blue dye. SN Applied Sciences 2 (5), 1–10.

Mahmud, H.N.M.E., Huq, A.O. and binti Yahya, R., 2016. The removal of heavy metal ions from wastewater/aqueous solution using polypyrrole-based adsorbents: a review. RSC Advances, 6 (18), pp.14778-14791.

Melo, B.C., Paulino, F.A., Cardoso, V.A., Pereira, A.G., Fajardo, A. R., Rodrigues, F.H., 2018. Cellulose nanowhiskers improve the methylene blue adsorption capacity of chitosan-g-poly (acrylic acid) hydrogel. Carbohydr. Polym. 181, 358–367.

Minisy, I.M., Salahuddin, N.A., Ayad, M.M., 2021. Adsorption of methylene blue onto chitosan–montmorillonite/polyaniline nanocomposite. Appl. Clay Sci. 203, 105993.

Mittal, H., Al Alili, A., Morajkar, P.P., Alhassan, S.M., 2021. GO crosslinked hydrogel nanocomposites of chitosan/carboxymethyl cellulose–A versatile adsorbent for the treatment of dyes contaminated wastewater. Int. J. Biol. Macromol. 167, 1248–1261.

Mittal, H., Ray, S.S., Okamoto, M., 2016. Recent progress on the design and applications of polysaccharide-based graft copolymer hydrogels as adsorbents for wastewater purification. Macromol. Mater. Eng. 301 (5), 496–522.

Mohamed, R.R., Elella, M.H.A., Sabaa, M.W., 2017. Cytotoxicity and metal ions removal using antibacterial biodegradable hydrogels based on N-quaternized chitosan/poly (acrylic acid). Int. J. Biol. Macromol. 98, 302–313.

Ngwabebhoh, F.A., Gazi, M., Oladipo, A.A., 2016. Adsorptive removal of multi-azo dye from aqueous phase using a semi-IPN superabsorbent chitosan-starch hydrogel. Chem. Eng. Res. Des. 112, 274–288.

Okereafor, U., Makhatha, M., Mekuto, L., Uche-Okereafor, N., Sebola, T., Mavumengwana, V., 2020. Toxic metal implications on agricultural soils, plants, animals, aquatic life and human health. Int. J. Environ. Res. Public Health 17 (7), 2204.

Pashaei-Fakhri, S., Peighambardoust, S.J., Foroutan, R., Arsalani, N., Ramavandi, B., 2021. Crystal violet dye sorption over acrylamide/graphene oxide bonded sodium alginate nanocomposite hydrogel. Chemosphere 270, 129419.

Paulino, A.T., Belfiore, L.A., Kubota, L.T., Muniz, E.C., Almeida, V.C., Tambourgi, E.B., 2011. Effect of magnetite on the adsorption

behavior of Pb (II), Cd (II), and Cu (II) in chitosan-based hydrogels. Desalination 275 (1–3), 187–196.

Pavithra, S., Thandapani, G., Sugashini, S., Sudha, P.N., Alkhamis, H.H., Alrefaei, A.F., Almutairi, M.H., 2021. Batch adsorption studies on surface tailored chitosan/orange peel hydrogel composite for the removal of Cr (VI) and Cu (II) ions from synthetic wastewater. Chemosphere 271, 129415.

Parshi, N., Pan, D., Dhavle, V., Jana, B., Maity, S., Ganguly, J., 2019. Fabrication of lightweight and reusable salicylaldehyde functionalized chitosan as adsorbent for dye removal and its mechanism. Int. J. Biol. Macromol. 141, 626–635.

Pérez-Álvarez, L., Ruiz-Rubio, L., Lizundia, E., Vilas-Vilela, J.L., 2019. Polysaccharide-based superabsorbents: synthesis, properties, and applications. Cham, Switzerland, Springer Nature, pp. 1393–1431.

Pérez-Calderón, J., Santos, M.V., Zaritzky, N., 2020. Synthesis, characterization and application of cross-linked chitosan/oxalic acid hydrogels to improve azo dye (Reactive Red 195) adsorption. React. Funct. Polym. 155, 104699.

Quesada, H.B., de Araujo, T.P., Vareschini, D.T., de Barros, M.A.S.D., Gomes, R.G. and Bergamasco, R., 2020. Chitosan, alginate and other macromolecules as activated carbon immobilizing agents: a review on composite adsorbents for the removal of water contaminants. International Journal of Biological Macromolecules.

Rashid, S., Shen, C., Yang, J., Liu, J., Li, J., 2018. Preparation and properties of chitosan–metal complex: some factors influencing the adsorption capacity for dyes in aqueous solution. J. Environ. Sci. 66, 301–309.

Reghioua, A., Barkat, D., Jawad, A.H., Abdulhameed, A.S., Khan, M.R., 2021. Synthesis of Schiff's base magnetic crosslinked chitosan-glyoxal/ZnO/Fe3O4 nanoparticles for enhanced adsorption of organic dye: modeling and mechanism study. Sustain. Chem. Pharm. 20, 100379.

Sarayu, K., Sandhya, S., 2012. Current technologies for biological treatment of textile wastewater – a review. Appl. Biochem. Biotechnol. 167 (3), 645–661.

Sasi, P.C., Alinezhad, A., Yao, B., Kubátová, A., Golovko, S.A., Golovko, M.Y., Xiao, F., 2021. Effect of granular activated carbon and other porous materials on thermal decomposition of per-and polyfluoroalkyl substances: Mechanisms and implications for water purification. Water Res. 200, 117271.

Schweitzer, L., Noblet, J., 2018. Water contamination and pollution. In: Green chemistry. Elsevier, pp. 261–290.

Seow, T.W., Lim, C.K., Nor, M.H.M., Mubarak, M.F.M., Lam, C.Y., Yahya, A., Ibrahim, Z., 2016. Review on wastewater treatment technologies. Int. J. Appl. Environ. Sci 11 (1), 111–126.

Shalla, A.H., Yaseen, Z., Bhat, M.A., Rangreez, T.A., Maswal, M., 2019. Recent review for removal of metal ions by hydrogels. Sep. Sci. Technol. 54 (1), 89–100.

Sharma, A.K., Kaith, B.S., Tanwar, V., Bhatia, J.K., Sharma, N., Bajaj, S., Panchal, S., 2019. RSM-CCD optimized sodium alginate/gelatin based ZnS-nanocomposite hydrogel for the effective removal of biebrich scarlet and crystal violet dyes. Int. J. Biol. Macromol. 129, 214–226.

Shehzad, H., Ahmed, E., Sharif, A., Din, M.I., Farooqi, Z.H., Nawaz, I., Bano, R., Iftikhar, M., 2020. Amino-carbamate moiety grafted calcium alginate hydrogel beads for effective biosorption of Ag (I) from aqueous solution: economically-competitive recovery. Int. J. Biol. Macromol. 144, 362–372.

Shen, W., An, Q.D., Xiao, Z.Y., Zhai, S.R., Hao, J.A., Tong, Y., 2020. Alginate modified graphitic carbon nitride composite hydrogels for efficient removal of Pb (II), Ni (II) and Cu (II) from water. Int. J. Biol. Macromol. 148, 1298–1306.

Silverstein, M.S., 2020. Interpenetrating polymer networks: so happy together? Polymer 207, 122929.

Steinegger, A., Wolfbeis, O.S., Borisov, S.M., 2020. Optical sensing and imaging of pH values: spectroscopies, materials, and applications. Chem. Rev. 120 (22), 12357–12489.

Sweetman, M.J., May, S., Mebberson, N., Pendleton, P., Vasilev, K., Plush, S.E., Hayball, J.D., 2017. Activated carbon, carbon nanotubes and graphene: materials and composites for advanced water purification. C 3 (2), 18.

Tao, E., Ma, D., Yang, S., Hao, X., 2020. Graphene oxide-montmorillonite/sodium alginate aerogel beads for selective adsorption of methylene blue in wastewater. J. Alloy. Compd. 832, 154833.

Tao, X., Wang, S., Li, Z., Zhou, S., 2021. Green synthesis of network nanostructured calcium alginate hydrogel and its removal performance of Cd2+ and Cu2+ ions. Mater. Chem. Phys. 258, 123931.

Tang, S., Yang, J., Lin, L., Peng, K., Chen, Y., Jin, S., Yao, W., 2020. Construction of physically crosslinked chitosan/sodium alginate/calcium ion double-network hydrogel and its application to heavy metal ions removal. Chem. Eng. J. 393, 124728.

Thakur, S., Pandey, S., Arotiba, O.A., 2016. Development of a sodium alginate-based organic/inorganic superabsorbent composite hydrogel for adsorption of methylene blue. Carbohydr. Polym. 153, 34–46.

Thakur, S., Chaudhary, J., Kumar, V., Thakur, V.K., 2019. Progress in pectin based hydrogels for water purification: trends and challenges. J. Environ. Manage. 238, 210–223.

Tu, H., Yu, Y., Chen, J., Shi, X., Zhou, J., Deng, H., Du, Y., 2017. Highly cost-effective and high-strength hydrogels as dye adsorbents from natural polymers: chitosan and cellulose. Polym. Chem. 8 (19), 2913–2921.

Van Tran, V., Park, D., Lee, Y.C., 2018. Hydrogel applications for adsorption of contaminants in water and wastewater treatment. Environ. Sci. Pollut. Res. 25 (25), 24569–24599.

Verma, A., Thakur, S., Mamba, G., Gupta, R.K., Thakur, P., Thakur, V.K., 2020. Graphite modified sodium alginate hydrogel composite for efficient removal of malachite green dye. Int. J. Biol. Macromol. 148, 1130–1139.

Vieira, R.M., Vilela, P.B., Becegato, V.A., Paulino, A.T., 2018. Chitosan-based hydrogel and chitosan/acid-activated montmorillonite composite hydrogel for the adsorption and removal of Pb+2 and Ni+2 ions accommodated in aqueous solutions. J. Environ. Chem. Eng. 6 (2), 2713–2723.

Wang, Y., Zhang, X., Qiu, D., Li, Y., Yao, L., Duan, J., 2018a. Ultrasonic assisted microwave synthesis of poly (Chitosan-co-gelatin)/polyvinyl pyrrolidone IPN hydrogel. Ultrason. Sonochem. 40, 714–719.

Wang, W., Ni, J., Chen, L., Ai, Z., Zhao, Y., Song, S., 2020. Synthesis of carboxymethyl cellulose-chitosan-montmorillonite nanosheets composite hydrogel for dye effluent remediation. Int. J. Biol. Macromol. 165, 1–10.

Wang, W., Zhao, Y., Bai, H., Zhang, T., Ibarra-Galvan, V., Song, S., 2018b. Methylene blue removal from water using the hydrogel beads of poly (vinyl alcohol)-sodium alginate-chitosan-montmorillonite. Carbohydr. Polym. 198, 518–528.

Wang, W.B., Huang, D.J., Kang, Y.R., Wang, A.Q., 2013. One-step in situ fabrication of a granular semi-IPN hydrogel based on chitosan and gelatin for fast and efficient adsorption of Cu2+ ion. Colloids Surf., B 106, 51–59.

Wu, S., Wang, F., Yuan, H., Zhang, L., Mao, S., Liu, X., Alharbi, N.S., Rohani, S., Lu, J., 2018. Fabrication of xanthate-modified chitosan/poly (N-isopropylacrylamide) composite hydrogel for the selective adsorption of Cu (II), Pb (II) and Ni (II) metal ions. Chem. Eng. Res. Des. 139, 197–210.

Wu, J., Cheng, X., Li, Y., Yang, G., 2019. Constructing biodegradable nanochitin-contained chitosan hydrogel beads for fast and efficient removal of Cu (II) from aqueous solution. Carbohydr. Polym. 211, 152–160.

Yadav, S., Asthana, A., Singh, A.K., Chakraborty, R., Vidya, S.S., Susan, M.A.B.H., Carabineiro, S.A., 2021. Adsorption of cationic dyes, drugs and metal from aqueous solutions using a polymer composite of magnetic/β-cyclodextrin/activated charcoal/Na algi-

nate: Isotherm, kinetics and regeneration studies. J. Hazard. Mater. 409, 124840.

Yi, X., Sun, F., Han, Z., Han, F., He, J., Ou, M., Gu, J., Xu, X., 2018. Graphene oxide encapsulated polyvinyl alcohol/sodium alginate hydrogel microspheres for Cu (II) and U (VI) removal. Ecotoxicol. Environ. Saf. 158, 309–318.

Yu, J., Wang, Y., He, Y., Gao, Y., Hou, R., Ma, J., Zhang, L., Guo, X., Chen, L., 2021. Calcium ion-sodium alginate double cross-linked graphene oxide nanofiltration membrane with enhanced stability for efficient separation of dyes. Sep. Purif. Technol. 276, 119348.

Yu, K., Ho, J., McCandlish, E., Buckley, B., Patel, R., Li, Z., Shapley, N.C., 2013. Copper ion adsorption by chitosan nanoparticles and alginate microparticles for water purification applications. Colloids Surf., A 425, 31–41.

Zhu, H.Y., Fu, Y.Q., Jiang, R., Yao, J., Xiao, L., Zeng, G.M., 2012. Novel magnetic chitosan/poly (vinyl alcohol) hydrogel beads: Preparation, characterization and application for adsorption of dye from aqueous solution. Bioresour. Technol. 105, 24–30.

Zhou, J., Hao, B., Wang, L., Ma, J., Cheng, W., 2017. Preparation and characterization of nano-TiO2/chitosan/poly (N-isopropylacrylamide) composite hydrogel and its application for removal of ionic dyes. Sep. Purif. Technol. 176, 193–199.

Zhou, C., Tong, D. and Yu, W., 2019. Smectite Nanomaterials: Preparation, Properties, and Functional Applications. In: Nanomaterials from Clay Minerals (pp. 335-364). Elsevier.

Zhao, N., Bitar, H.A., Zhu, Y., Xu, Y., Shi, Z., 2020. Synthesis of polymer grafted starches and their flocculation properties in clay suspension. Minerals 10 (12), 1054.

Zhao, J., Zou, Z., Ren, R., Sui, X., Mao, Z., Xu, H., Zhong, Y., Zhang, L., Wang, B., 2018. Chitosan adsorbent reinforced with citric acid modified β-cyclodextrin for highly efficient removal of dyes from reactive dyeing effluents. Eur. Polym. J. 108, 212–218.

Zhang, H., Omer, A.M., Hu, Z., Yang, L.Y., Ji, C., Ouyang, X.K., 2019. Fabrication of magnetic bentonite/carboxymethyl chitosan/sodium alginate hydrogel beads for Cu (II) adsorption. Int. J. Biol. Macromol. 135, 490–500.

Ziarani, G.M., Moradi, R., Lashgari, N., Kruger, H.G., 2018. Metal-free synthetic Organic Dyes. Elsevier.

Zoratto, N., Matricardi, P., 2018. Semi-IPNs and IPN-based hydrogels. Polymeric Gels, 91–124.

Zubair, M., Ullah, A., 2021. Biopolymers in environmental applications: industrial wastewater treatment. Biopolym. Their Ind. Appl., 331–349